

Laser-driven Propulsion of Multilayer Graphene Oxide Flakes

Supporting Information

Chengbing Qin, Zhixing Qiao, Wenjun He, Guofeng Zhang, Ruiyun Chen, Yan Gao,*

Liantuan Xiao, and Suotang Jia*

State Key Laboratory of Quantum Optics and Quantum Optics Devices, Institute of Laser Spectroscopy, Shanxi University, Taiyuan, Shanxi 030006, China.

Collaborative Innovation Center of Extreme Optics, Shanxi University, Taiyuan, Shanxi 030006, China.

Content

1. Preparation of GO suspension	2
2. Optical imaging of GO flakes	4
3. Experimental setup of confocal system.....	5
4. GO propulsion driven by CW laser irradiation	8
5. Calculations of centres of GO flakes.....	9
6. Propulsion of GO flakes driven by femtosecond laser irradiation	12
7. Investigations of the producing gases	13
8. AFM and SEM characterizations of GO flakes.....	15
References.....	17

1. Preparation of GO suspension

The original GO suspension, purchased from Nanjing XFNANO materials Tech Co., Ltd., was synthesized by modified Hummers methods.^{S1-S3} The detailed process was as follows:

Typically, graphite powder (2.0 g) was mixed with a mixture of H₂SO₄ (98%, 100 mL), KMnO₄ (10.0 g), and NaNO₃ (4.0 g) in ice bath. After removing the ice bath, the mixture was transferred to a water bath with temperature of 35 °C and stirred for about 1 hour. Then Milli-Q water (100 mL) was added to the mixture. After successively stirring for 0.5 hour at the temperature of 90 °C, Milli-Q water (150 mL) and H₂O₂ (30%, 6 mL) were added into the mixture slowly. After the color of the mixture turning from dark brown to light brown, the mixture was centrifuged (4000 rpm) and washed with HCl (5%) and Milli-Q water for several times. After filtration and vacuum drying at room temperature for 2 days, the GO powder with the color of dark brown was obtained.

To get the GO suspension with the concentration of 0.5 mg/mL, the GO powder (100 mg) was re-dispersed into the Milli-Q water (200 mL) by ultrasonic treatment (350W@33 kHz for 2 hours). In this experiment, the suspension was further diluted to 1×10^{-2} mg/mL by adding the Milli-Q water.

The diluted suspension shows a yellow color, as shown in Figure S1a. To achieve the thick multilayer GO flakes, the original diluted GO suspension was reduced by Hg lamp irradiation with the power of 500 W (Figure S1c). The color of processing suspension was turning from yellow to dark as the increasing of irradiation duration, as shown in Figure S1a. Meanwhile, lots of small suspended solids in dark was formed during lamp irradiation, which were the re-aggregation of reduced GO. Figure S2 presents the Raman spectra and FTIR spectra of the original and processing GO suspension, respectively. According to the slight increase of I_D/I_G ratio and the decrease of the O-H stretching vibration (2800-3600 cm⁻¹),^{S4-S7} the processing GO has been slightly reduced.

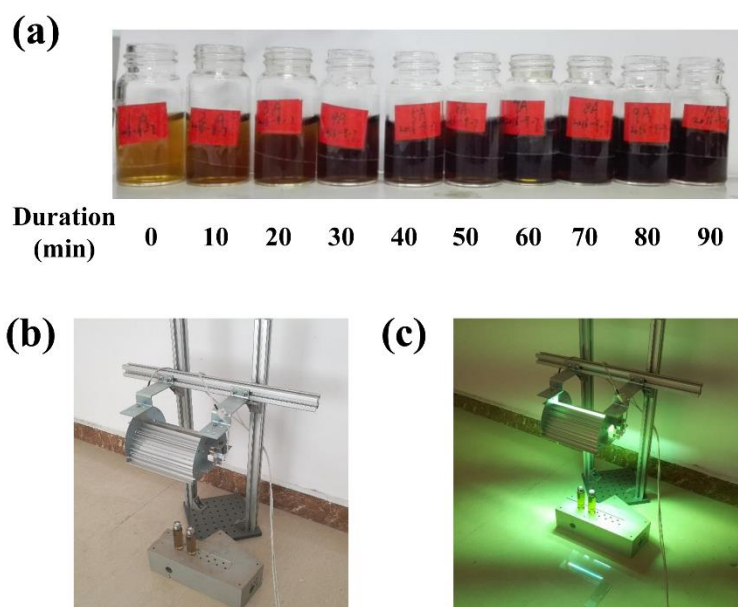


Figure S1. (a) GO suspension after irradiation with Hg lamp (500 W) with different durations. (b), (c) The photographs with Hg lamp off and on, respectively.

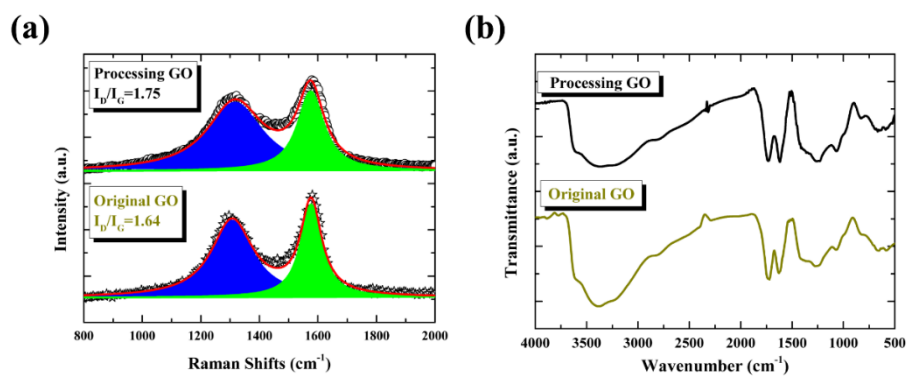


Figure S2. Raman and FTIR spectra of the original and processing GO suspension.

2. Optical imaging of GO flakes

The GO suspension with the irradiation duration of 10 min was selected to prepare the GO flakes by drop-coating the suspension (100 μL) on the glass coverslip. The optical images (transmission imaging under light of halogen lamp) of the samples prepared by original and processing GO suspension were presented in Figure S3, respectively. Note that the optical image for the original GO (Figure S3a) presents almost uniform color with few dark areas (marked as circle) on the surface. The big ratio (>99%) and small scale (1-5 μm) of monolayer GO results in the uniform and thin film. In the case, the color of GO film cannot be distinctly observed. On the other hand, the optical image for the processing GO presents many dark areas on the surface. These dark areas are the GO flakes with different scales. It can be found that these flakes are separated with each other. The background with blue color is glass coverslip. In the case, the glass coverslip is like “Ocean”, while the GO flakes is like “Island”. Due to the strong absorption of GO flakes, we can clearly determine the “island-like structure” from the background.

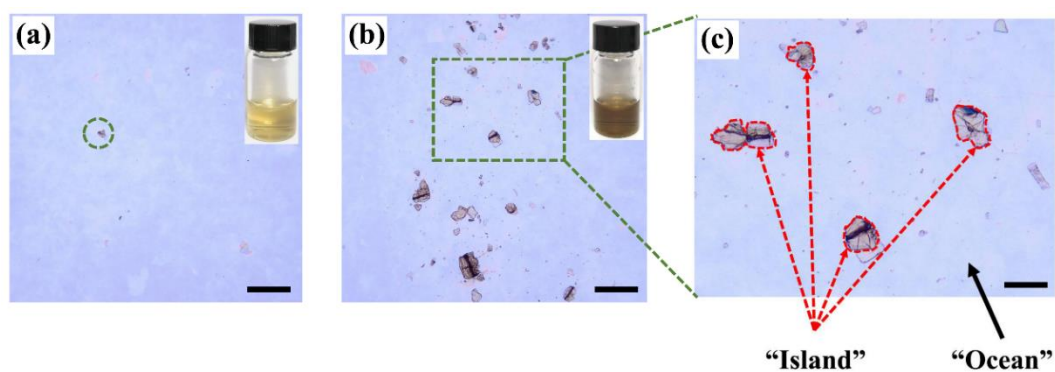


Figure S3. Optical images of prepared samples. (a) GO film prepared by original GO suspension. Scale bar: 100 μm . (b) GO flakes prepared by processing GO suspension. Scale bar: 100 μm . (c) “Island-like structure” on the optical image. Scale bar: 30 μm . Insets in (a) and (b) are the photographs of original and processing GO suspensions.

3. Experimental setup of confocal system

The propulsion of GO flakes was driven by femtosecond laser, and the propulsion trajectories were visualized by confocal fluorescence images. The fluorescence of GO flakes excited by the femtosecond laser was extremely weak in our detection region (400-700 nm), as shown in Figure S4. Thus, a 405 nm continuum-wave (CW) laser was used to locate the GO flakes through fluorescence image, of which the fluorescence was strong enough to observe the propulsion trajectory. The spectra excited by 405 nm CW laser are in good agreement with the reported literature,^{S8} where the GO was also excited by ultraviolet laser. The fluorescence spectra of different areas have also been presented in Figure S5. Note that the background noise (labeled as 4) can be ignored in the experiment. Beyond the fluorescence imaging, the optical imaging (transmission imaging) can also be used to visualize the propulsion trajectory, however, in the case, the variation in their fluorescence cannot be achieved synchronously.

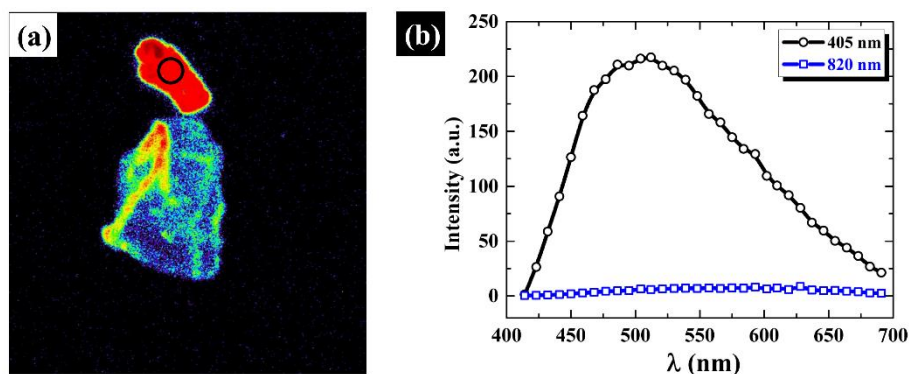


Figure S4. GO's spectra excited by 405 and 820 nm. (a) Fluorescence imaging excited by 405 nm. The area marked as circle (\circ) was used to collect the fluorescence spectra. (b) Comparison of fluorescence spectra between two excitations.

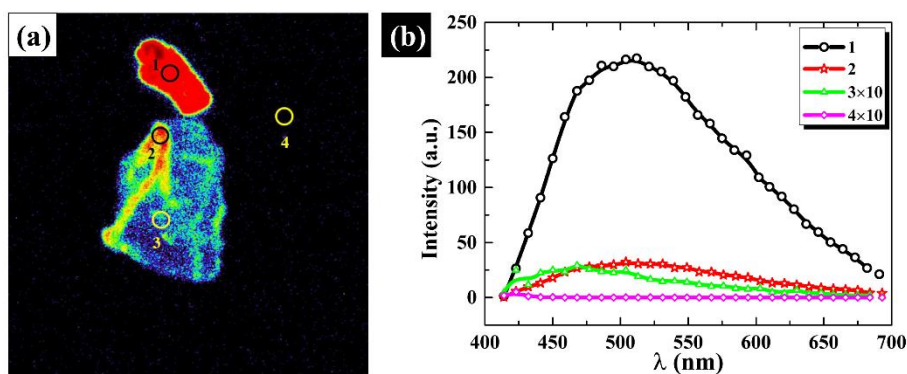


Figure S5. Comparison of fluorescence spectra between marked areas, excited by 405 nm CW laser.

Both laser irradiation and confocal fluorescence images were taken with a home-built scanning confocal microscope based on an inverted microscope (Nikon, TE2000-U).^{S9,S10} The schematic of experimental configuration was shown in Figure S6. The femtosecond laser at the center wavelength of 820 nm with the pulse width about 70 fs was employed to excite and propel the GO flakes at the repetition frequency of 80 MHz. The power of 405 nm CW laser used to visualize the GO sample was only 0.2 mW. Both femtosecond laser and CW laser were directed by dichroic mirrors (DM, Semrock, Di02-R405-25x36) towards an objective (OBJ, Nikon, 60 \times , 0.75 NA) to propel or excite the GO flakes. Fluorescence of GO flakes was collected by the same objective and passed through the DM, a notch filter and an emission filter (EmF, Semrock, FF01-496/LP-25) to block the back scattered laser light embedded in fluorescence. After passing through a 100 μ m spatial filter, the fluorescence was detected by an avalanche photon detector (APD, PerkinElmer, SPCM-AQR-15). The GO sample was placed on the piezoelectric nanometer translation stage (PZT-S, Tritor, 200/20SG). Confocal fluorescence image was acquired by raster scanning the GO sample in the focal plane, and the fluorescence intensity was recorded for each imaging pixel. The integration time for each pixel was set to 1 ms. A monochromator was also used to obtain the fluorescence spectrum.

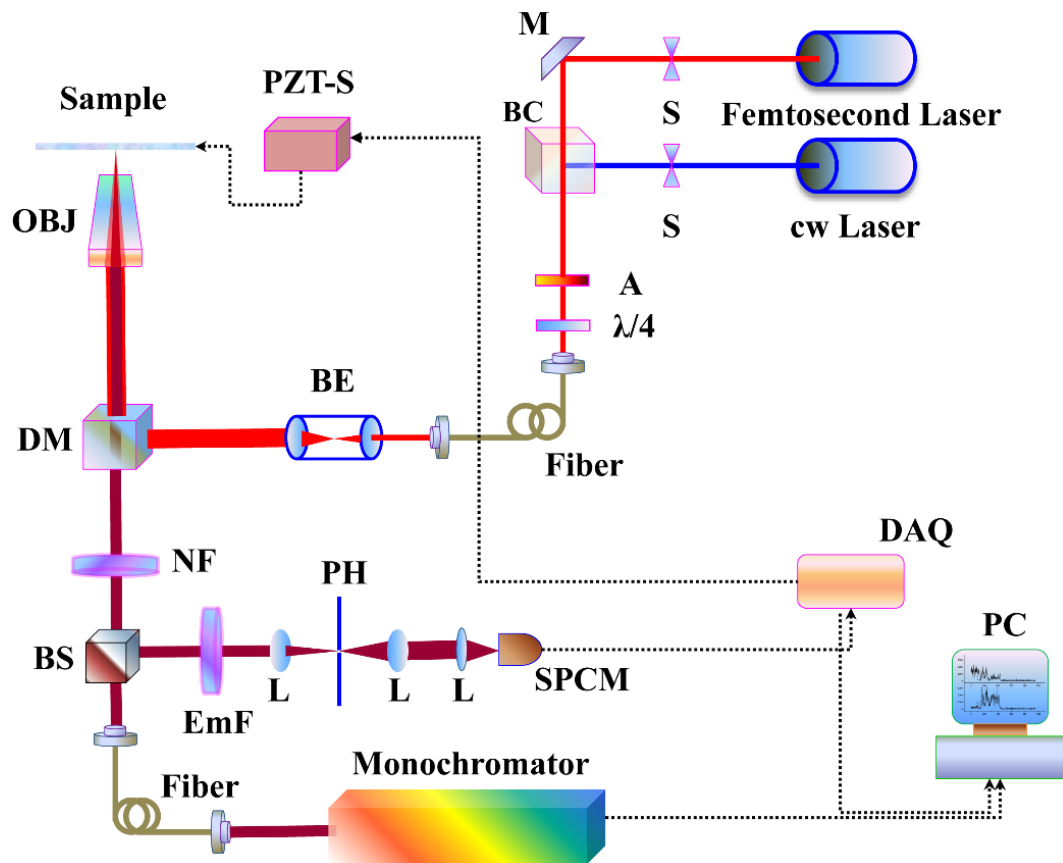


Figure S6. Schematic depiction of experimental setup. **S**: shutter; **M**: mirror; **BC**: beam combiner; **A**: attenuator; **BE**: beam expander; **DM**: dichroic mirror; **OBJ**: objective; **PZT-S**: piezoelectric nanometer translation stage; **NF**: notch filter; **BS**: beam splitter; **EmF**: Emission filter; **L**: lens; **PH**: pinhole; **SPCM**: single photon counting module; **DAQ**: data acquisition card; **PC**: personal computer. The dashed lines denote **BNC** cables.

4. GO propulsion driven by CW laser irradiation

The GO flakes were also irradiated by 405 nm CW laser with the same power (210 mW) and irradiation duration (3 μ s) following each femtosecond laser irradiation. After the CW laser irradiation, the GO trajectories were also visualized by 405 nm laser again with extremely weak power (0.2 mW). Figure S7 presents the fluorescence image arrays of the GO flakes after CW laser irradiation between the 10th and the 11th time femtosecond laser irradiation. No obvious displacements can be found after 30 times CW laser irradiation, which provides the proof that the CW laser cannot propel the GO flakes effectively.

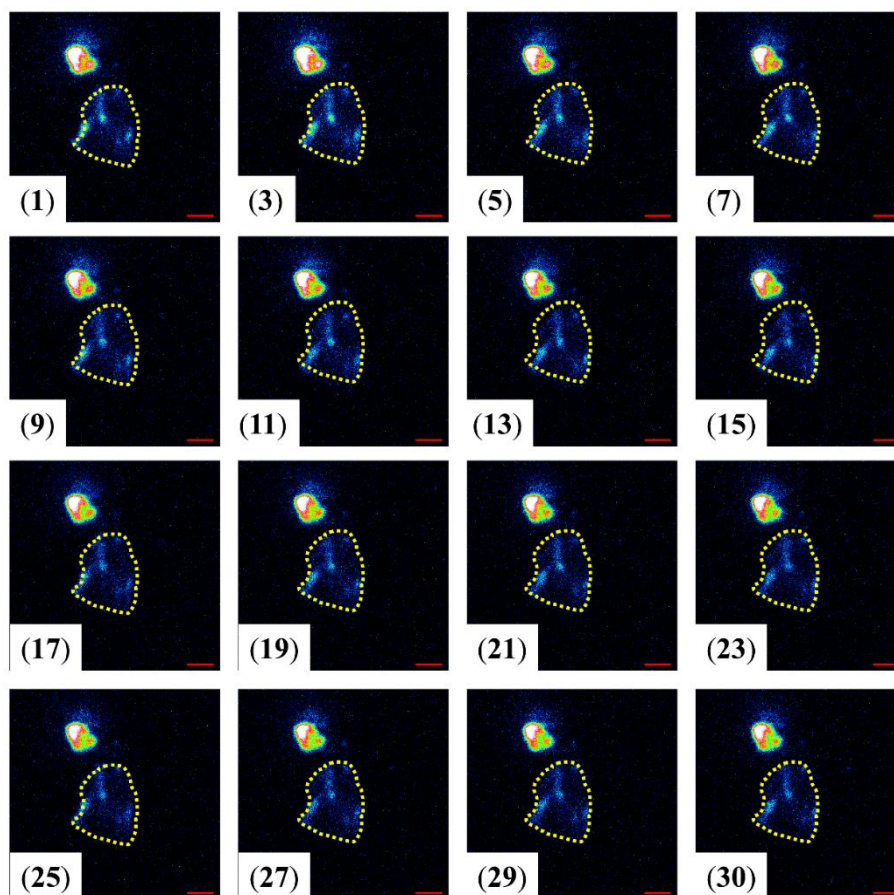


Figure S7. Sequences of confocal fluorescence images for the two GO flakes after 405 nm CW laser irradiation, and the ordinal numbers on the bottom left denote the times of irradiation. The irradiation power is 210 mW with duration time of 3 μ s. The region of bottom flake is heighted by yellow dashed lines. Scale bar: 10 μ m.

5. Calculations of centres of GO flakes

In order to quantify the displacements, we define the geometric boundary of GO flakes through fluorescence threshold, and calculate the geometric centers. Considering the quite different fluorescence intensity for the upper and bottom flakes, we divide them into two parts, as shown in Figure S8. Their threshold values are chosen according to the fluorescence intensity around the edge of the flakes, respectively. Take the upper one as an example, when the threshold value of the fluorescence intensity is setting as $I_{\text{thr}} = 8.0$, as shown in Figure S9, only the pixels with the fluorescence intensity in the region of 7.95-8.05 would be displayed. For each pixel, they has a coordinate as (x_i, y_i) , where x_i and y_i are the corresponding number for the image pixels. Combining with fluorescence image, the outermost pixel was selected to link together, thus the edge of the GO flakes can be determined. The geometric centre (X, Y) of the flake can be calculated as following:

$$X = \frac{1}{N} \sum_{i=1}^N x_i, \quad Y = \frac{1}{N} \sum_{i=1}^N y_i$$

Note that some pixels with the intensity also in the region of 7.95-8.05 would be displayed, but far from the boundary of fluorescence image. These pixels should be excluded from the calculations.

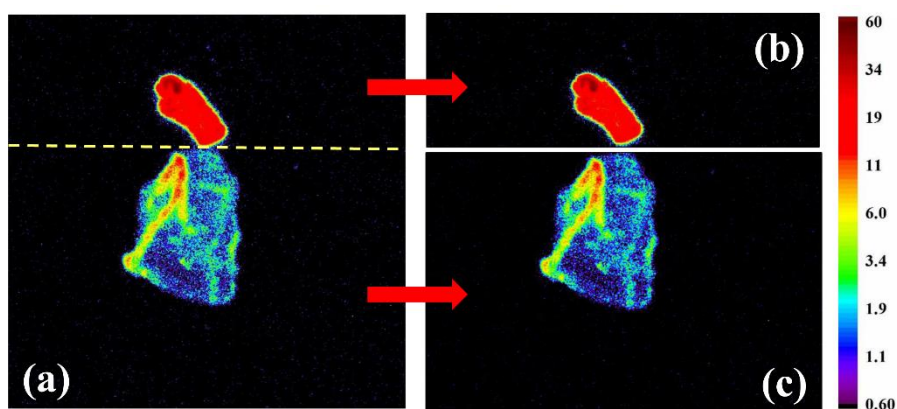


Figure S8. (a) Confocal fluorescence image of GO flakes. The two flakes are divided into two parts by the yellow dash line. (b), (c) are the fluorescence images for the upper and bottom flakes, respectively.

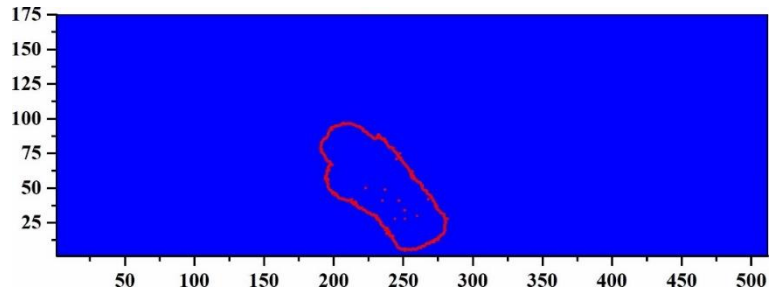


Figure S9. The selected pixels when $I_{\text{thr}} = 8.0$. The outermost pixels is linked together to build the edge of GO flake.

Figure S10a displays six conditions of selected pixels for the upper flake when I_{thr} is set as 3.0, 4.0, 5.0, 6.0, 7.0, and 8.0, respectively. Similar shape can be determined for these six conditions. The calculated centers for them have also been presented in Figure S10b. One can find that the deviation arising from different thresholds can be ignored.

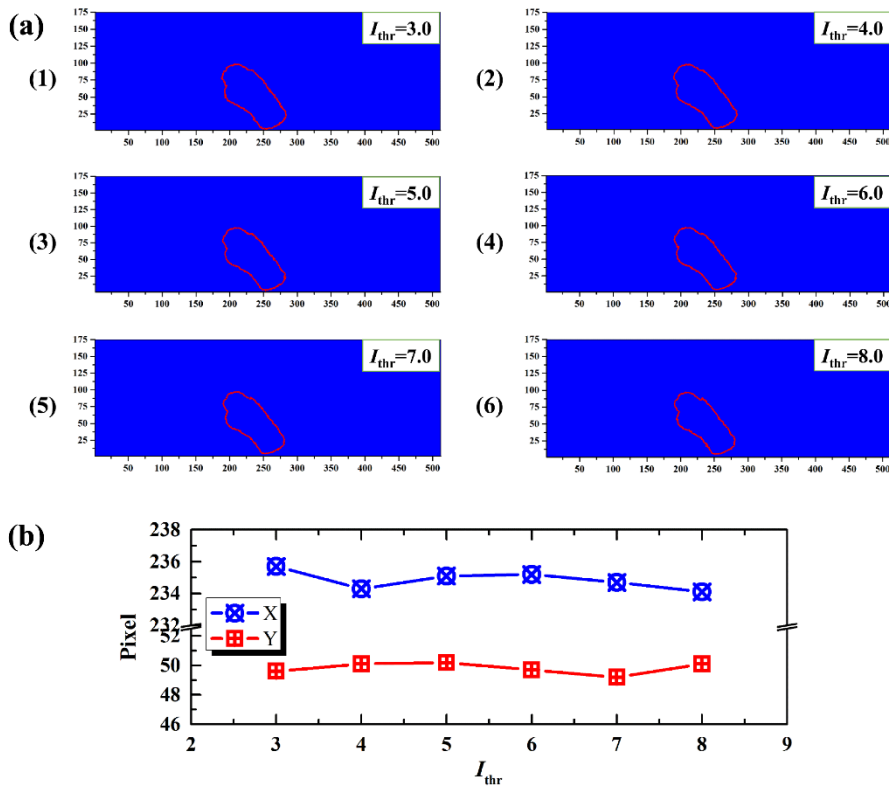


Figure S10. (a) The selected pixels for $I_{\text{thr}}=3.0, 4.0, 5.0, 6.0, 7.0,$ and $8.0,$ respectively. (b) The calculated values for X and Y varied as thresholds.

Figure S11a displays four conditions of selected pixels for the bottom flake when I_{thr} is set as 1.5, 2.0, 2.5, and 3.0, respectively. Many pixels outside the boundary of fluorescence can be found for the low threshold. In this condition, large threshold is more suitable.

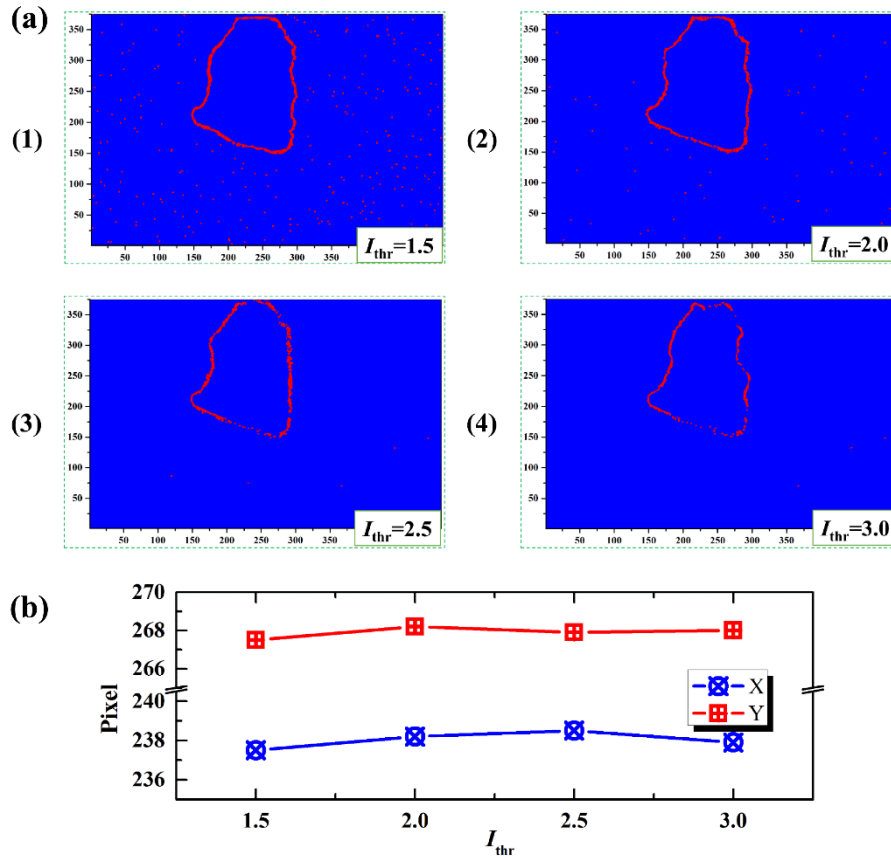


Figure S11. (a) The selected pixels for $I_{thr} = 1.5, 2.0, 2.5,$ and $3.0,$ respectively. (b) The calculated values for X and Y varied as threshold.

6. Propulsion of GO flakes driven by femtosecond laser irradiation

We also observed another GO flakes with propulsion driven by femtosecond laser irradiation, as following:

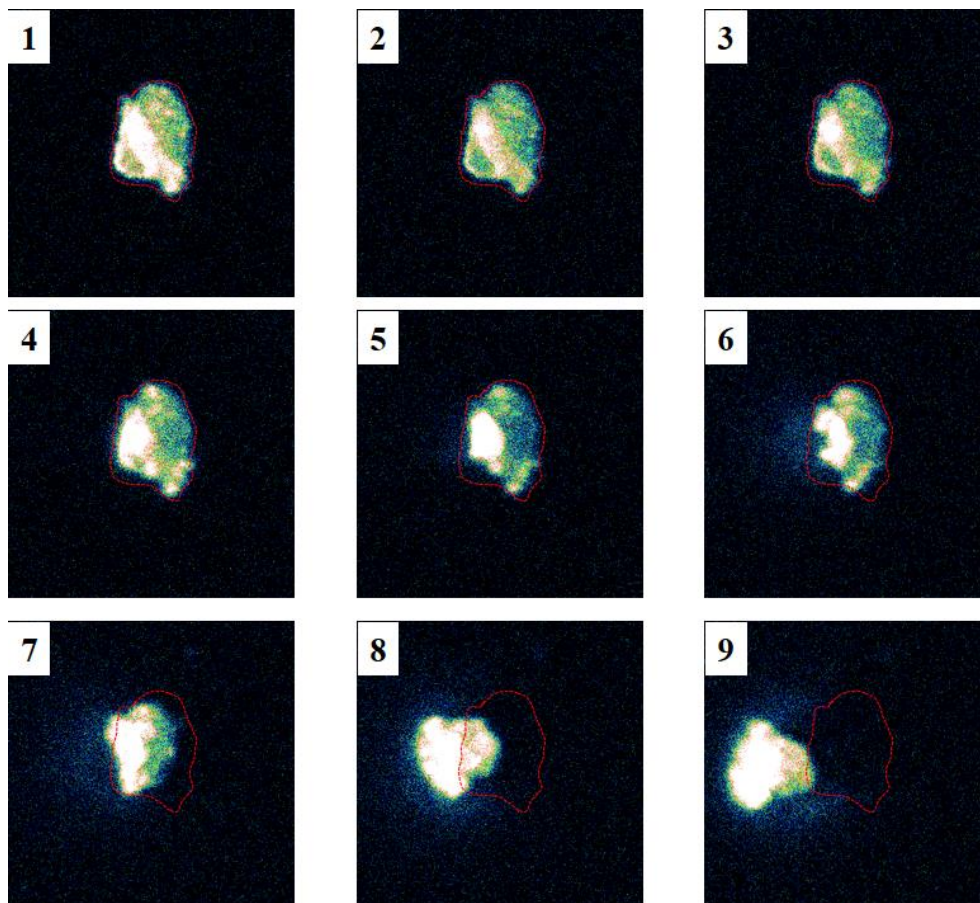


Figure S12. Sequences of confocal fluorescence images for the GO flake after femtosecond laser irradiation, the ordinal numbers on the top right denote the times of irradiation. The red dash lines are used to mark the original shape and location of the GO flake.

7. Investigations of the producing gases

We have confirmed the gas ejection through irradiating the bulk GO materials in a vacuum chamber. In the proposed mechanism, we suggest that the main species in the producing gases are H₂O, CO₂, CO and some small organic compounds. To further determine the exact chemical structures of these species, we filled the chamber with pure Nitrogen (~400 torr) and investigated the producing gases by quartz enhanced photoacoustic spectroscopy (QEPAS). The experimental setup can be found in the previous works.^{S11,S12} Particularly, the absorption line centered at 7306.75 cm⁻¹ (according to HITRAN database) was selected to measure the abundant of H₂O. A butterfly-package distributed feedback (DFB) laser with center wavelength of 1368 nm (7310 cm⁻¹) was used as the exciting light source. A commercially available quartz tuning fork (QTF) with a resonance frequency (f) of 32.755 kHz and quality factor (Q-factor) of 13534 was used as the photoacoustic transducer.

Figure S13a shows the QEPAS signal of H₂O absorption line at 7306.75 cm⁻¹. Apparently, without femtosecond laser irradiation, there is no obvious signal. While after irradiation with femtosecond laser, strong QEPAS signal can be observed, which confirms the presence of H₂O in producing gases undoubtedly. The presence of CO₂ has also been confirmed by QEPAS through absorption line centered at 6361.25 cm⁻¹. However, the CO and other species have not been determined, mainly resulting from the extremely low yields in the producing gases.

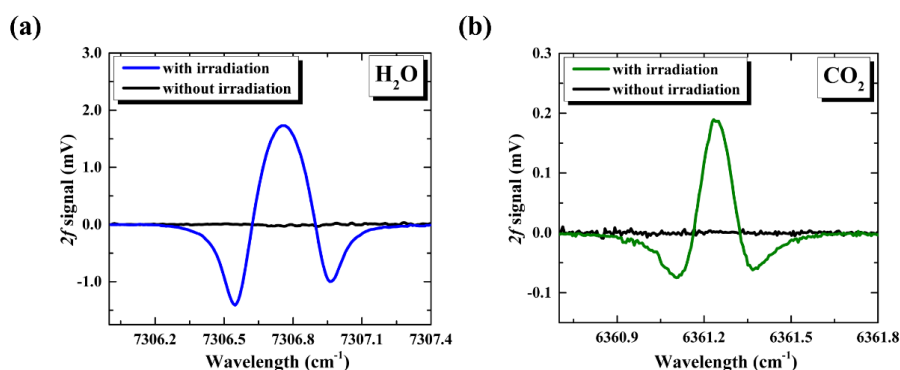


Figure S13. (a) QEPAS $2f$ signal at 7306.75 cm⁻¹ in Nitrogen (~400 torr) for H₂O absorption with and without femtosecond laser irradiation, respectively. (b) QEPAS $2f$ signal at 6361.25 cm⁻¹ in

Nitrogen (~400 torr) for CO₂ absorption with and without femtosecond laser irradiation, respectively.

On the other hand, gas chromatography mass spectrometry (GC-MS) has also been developed for the analysis of other species in the producing gases. Analytical measurements were conducted using a 6890N/5977 GC-MS system (Agilent Technology, USA).^{S13} Separations were performed using a 30 m length with 0.25 mm internal diameter with stationary phase of fused-silica capillary column coated with a 0.25 μm bonded film of 0.5% poly phenyl methyl silicon.^{S14} The producing gases were dissolved in dichloromethane (CH₂Cl₂), a 1 μL sample was injected in split mode with ratio of 10:1. The helium carrier gas flow was set to 1.0 mL/min. The temperature control program was 40 °C for 3 min, and then increasing to 280 °C at 5 °C/min. The temperature for the gasification compartment, the introduction port, ion source, and transmission line were set at 280, 250, 200, and 280 °C, respectively. In addition, the quality scanning area was from 40 to 500 amu.

A representative chromatographic output of the producing gases from the GC-MS is given in Figure S14, more than 50 compounds have been detected by GC-MS. However, in view of the complex chemical structure of GO materials and unknown reaction pathway, the exactly chemical structures for these compounds are still in analysis.

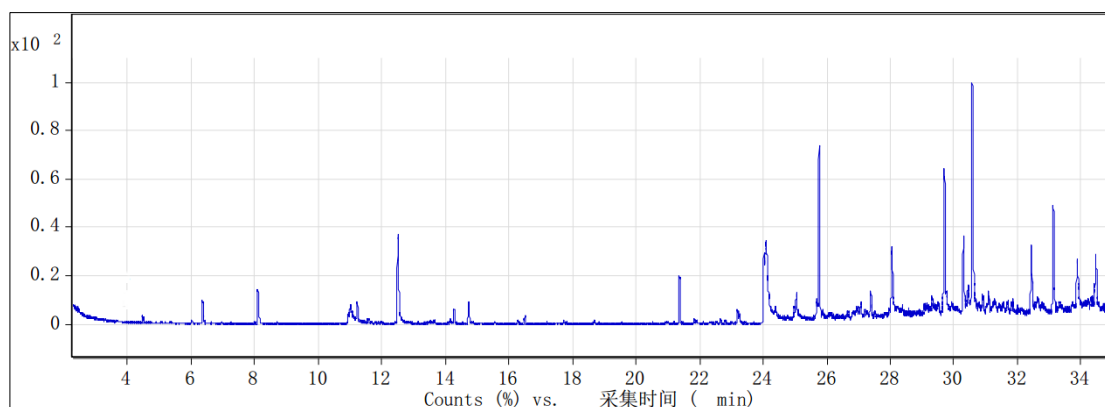


Figure S14. Gas chromatograms for the producing gases of GO film after irradiating by femtosecond laser.

8. AFM and SEM characterizations of GO flakes

To explore the presence of oxygen functional groups on the surface of GO, and also the variation of the oxygen functional groups before and after the femtosecond laser irradiation, the atomic force microscope (AFM, 5000N, JEOL, Japan) and scanning electron microscope (SEM, SU8010, Hitachi, Japan) with energy dispersive X-ray spectroscopy (EDS) were performed to characterize the morphologies of the prepared and irradiated GO samples.

Considering the thick thickness (~ 200 nm) of the prepared sample used in the experiment, which is hard to show the functional groups on the surface by AFM, we present the AFM images for monolayer GO before and after femtosecond laser irradiation. These monolayer GO films were prepared by spin-coating the original GO suspension on the glass coverslip. As shown in Figure S15a, the height of monolayer GO film prepared by original suspension is about 1.5 nm. After irradiating with femtosecond laser at power of 50 mW and duration of 3 ms, the height is reduced to ~ 1.1 nm, as shown in Figure S15b. The thicknesses of both prepared and irradiated samples are larger than that of graphene,^{S15} strongly hinting the presence of functional groups on the surface of GO. Comparing with the prepared sample, the decrease of thickness for the irradiated GO results from the elimination of some functional groups.

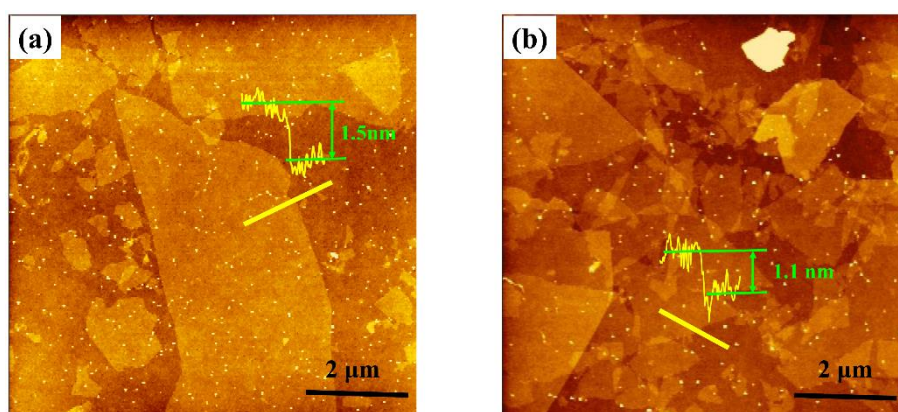


Figure S15. AFM images of the prepared and irradiated monolayer GO materials.

Figure S16 shows the SEM and EDS results of the prepared and irradiated GO flakes. In Figure S16a, the flake was compact, after irradiating with femtosecond laser,

the flakes become broken, and the edges show significant cracks. Some small fragments can also be found on the surface. From the results of EDS analysis (the inset tables give the descriptive statistics of the amount of elements in the surface of GO flakes), we can find that the main elements on the prepared samples are C and O, with a little of S. The abundant of O element strongly indicates the presence of oxygen functional groups. The presence of S element may result from the residue of H_2SO_4 , and also the sulfhydryl group (-SH) on the GO materials. After irradiating with femtosecond laser, the relative atomic content of O decreases from 24.30% to 14.76%, further revealing the reduction results.

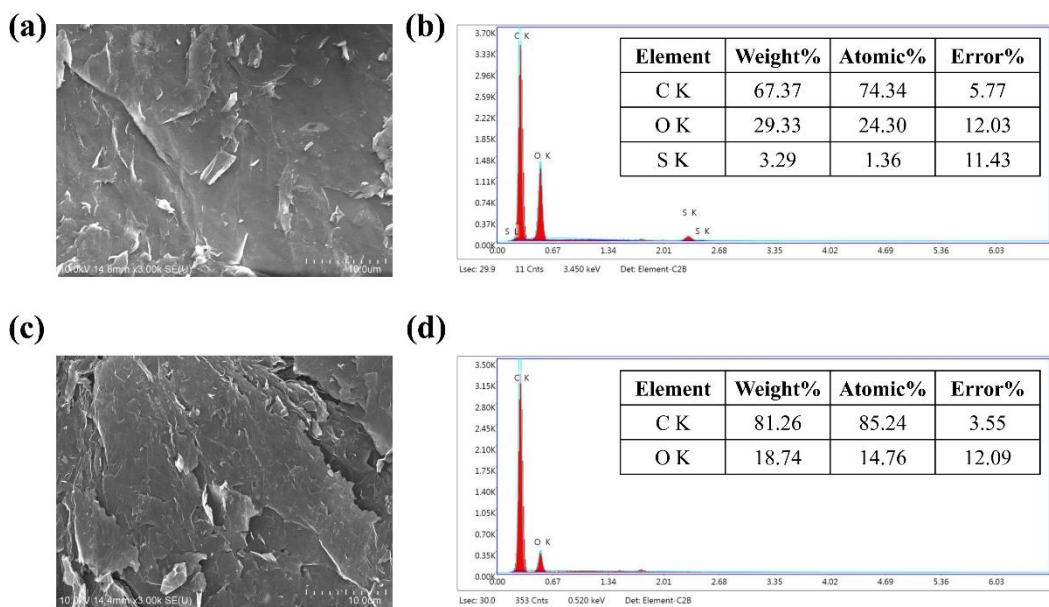


Figure S16. SEM and EDS results of GO flakes. (a), (b) are the results for the prepared GO flakes. (c), (d) are the results for the irradiated GO flakes. The inset tables are the descriptive statistics of the amount of elements on the surface of GO flakes.

References

- S1. S. Bai, X. Shen, X. Zhong, Y. Liu, G. Zhu, X. Xu and K. Chen, *Carbon*, 2012, **50**, 2337-2346.
- S2. J. Li, S. Zhang, C. Chen, G. Zhao, X. Yang, J. Li and X. Wang, *ACS Appl. Mater. Interfaces*, 2012, **4**, 4991-5000.
- S3. T. Liu, Y. Li, Q. Du, J. Sun, Y. Jiao, G. Yang, Z. Wang, Y. Xia, W. Zhang, K. Wang, H. Zhu and D. Wu, *Colloids Surf. B Biointerfaces*, 2012, **90**, 197-203.
- S4. F. Liu, H. D. Ha, D. J. Han and T. S. Seo, *Small*, 2013, **9**, 3410-3414.
- S5. J. Chen, B. Yao, C. Li and G. Shi, *Carbon*, 2013, **64**, 225-229.
- S6. H. Feng, R. Cheng, X. Zhao, X. Duan and J. Li, *Nat. Commun.*, 2013, **4**, 1539.
- S7. Q. Zhang, H. Zheng, Z. Geng, S. Jiang, J. Ge, K. Fan, S. Duan, Y. Chen, X. Wang and Y. Luo, *J. Am. Chem. Soc.*, 2013, **135**, 12468-12474.
- S8. G. Eda, Y. Y. Lin, C. Mattevi, H. Yamaguchi, H. A. Chen, I. S. Chen, C. W. Chen and M. Chhowalla, *Adv. Mater.*, 2010, **22**, 505-509.
- S9. W. He, C. Qin, Z. Qiao, G. Zhang, L. Xiao and S. Jia, *Carbon*, 2016, **109**, 264-268.
- S10. H. T. Zhou, C. B. Qin, R. Y. Chen, G. F. Zhang, L. T. Xiao and S. T. Jia, *Appl. Phys. Lett.*, 2014, **105**, 153301.
- S11. X. Yin, L. Dong, H. Zheng, X. Liu, H. Wu, Y. Yang, W. Ma, L. Zhang, W. Yin, L. Xiao and S. Jia, *Sensors (Basel)*, 2016, **16**, 162.
- S12. H. Zheng, L. Dong, X. Liu, Y. Liu, H. Wu, W. Ma, L. Zhang, W. Yin and S. Jia, *Laser Phys.*, 2015, **25**, 125601.
- S13. C. Zhang, J. Li, Z. Chen and F. Cheng, *J. Chem. Technol. Biot.*, 2018, **93**, 112-120.
- S14. K. Khosravi and G. W. Price, *Microchem. J.*, 2015, **121**, 205-212.
- S15. C. J. Shearer, A. D. Slattery, A. J. Stapleton, J. G. Shapter and C. T. Gibson, *Nanotechnology*, 2016, **27**, 125704.